

Artificial Perovskite Multiple Quantum Well Optoelectronics

Sang-Hyun Chin^{1,*} 

¹SKKU Advanced Institute of Nanotechnology (SAINT), Sungkyunkwan University, Republic of Korea

Abstract: Metal halide perovskite-based photovoltaics and light-emitting diodes have exhibited a promising trajectory toward commercial viability, nearing the performance levels of them to the commercially established materials. A particularly encouraging avenue involves tailoring the various dimensions of perovskite materials, notably through the implementation of perovskite multiple quantum wells (MQWs), to amplify their potential in optoelectronic applications. This comprehensive review delves into recent breakthroughs in both self-assembled perovskite MQWs and artificially fabricated counterparts, elucidating their mechanisms and performance characteristics. By gathering and evaluating the very original and the latest research findings, this review aims to provide valuable insights into the underlying principles governing optical behaviors of perovskite MQWs as well as optoelectronic and photonic applications. Furthermore, it outlines prospective research pathways, delineating potential pathways for further exploration and optimization of perovskite MQW-based devices. Through this general evaluation on the recent advancements and prospects, this review contributes to advancing the understanding and application of perovskite materials in next-generation optoelectronic and photonic technologies.

Keywords: perovskites, multiple quantum wells, optoelectronics, light-emitting diodes, coherent emission

1. Introduction

Metal halide perovskites (MHPs) have risen as an outstanding candidate in photovoltaic and light-emitting applications and are nearing the commercialization [1–4]. For the recent progress on the MHP optoelectronics, researchers have employed multi-dimensional perovskites including morphological and molecular low dimension as depicted in Figure 1 [5].

Conventional MHPs include 3 ionic components forming ABX₃ structures, which are A⁺ (methylammonium cation, formamidinium cation, or cesium cation), B²⁺ (lead cation or Tin cation), and X⁻ (iodide anion, bromide anion, and chloride anion). To form morphological low-dimensional perovskites, this bulky 3D ABX₃ structure should become 2D platelet, 1D wire, or 0D dot by reducing the dimension yet maintaining ABX₃ component. However, for the molecular low-dimensional halide hybrids, metal halide BX₆⁴⁻ octahedra are defined as a 0D dot and the dimension can be defined by the confinement from nearby A-site cation. In recent publications with MHP optoelectronics employing low dimensions, both morphological and molecular types are introduced to improve the performances. However, the original works on MHP-related optoelectronics employing low dimension have not been properly highlighted and introduced. In this work, the reports which employed low-dimensional perovskites are reviewed, with special attention given to those utilizing multiple quantum well-like perovskites to highlight potential topics to pave the unseen way.

*Corresponding author: Sang-Hyun Chin, Department of Nano Science and Technology and Department of Nanoengineering, Sungkyunkwan University, Republic of Korea. Email: sanghyunchin@skku.edu

2. The Genesis and the Renaissance of Perovskite Multiple Quantum Wells

In 2009, a research team in Toin Yokohama University led by Prof. Miyasaka reported CH₃NH₃PbI₃ (MAPbI₃), a 3D perovskite material, for high-performance dye-sensitized solar cells which show photon-to-electron power conversion efficiency of 3.8% [6]. By this inspirational work, Prof. Park's group in Sungkyunkwan University and Prof. Snaith's group in University of Oxford individually reported the solid-state perovskite solar cells in 2012, opening the gate for the entire research field [7, 8]. Not only photovoltaic research field but also several more milestone with light-emitting applications were established in 2014. The University of Cambridge reported room temperature high-performing 3D perovskite light-emitting diodes (LEDs) and optically pumped lasers [9, 10].

These pioneering works have impressed researchers who are currently dedicating their efforts to MHPs; however, MHPs were already reported elsewhere showing some potential for optoelectronic and photonic applications. Already in 19th century, H. L. Wells could obtain cesium lead-halide salts, which are commonly used in these days, and reported in *Zeitschrift für anorganische Chemie* [11]. After a century, the research groups led by Prof. Saito (1994) and Prof. Mitzi (1999) published results with low temperature and room temperature operating perovskite LEDs (PeLEDs) [12, 13]. It is noteworthy that the form of perovskite employed in PeLEDs is 2D Ruddlesden-Popper perovskite (molecular 2 dimensional).

The work by Saito et al. spin-coated extremely thin (~10 nm) phenethylammonium lead iodide perovskite onto indium tin oxide substrate and sequentially evaporated 1,3-bis[2-(4-tert-butylphenyl)-1,3,4-oxadiazole-5-yl] benzene (OXD7) and metal

Figure 1
MHPs and perovskite-related materials with different dimensionalities at both morphological and molecular levels

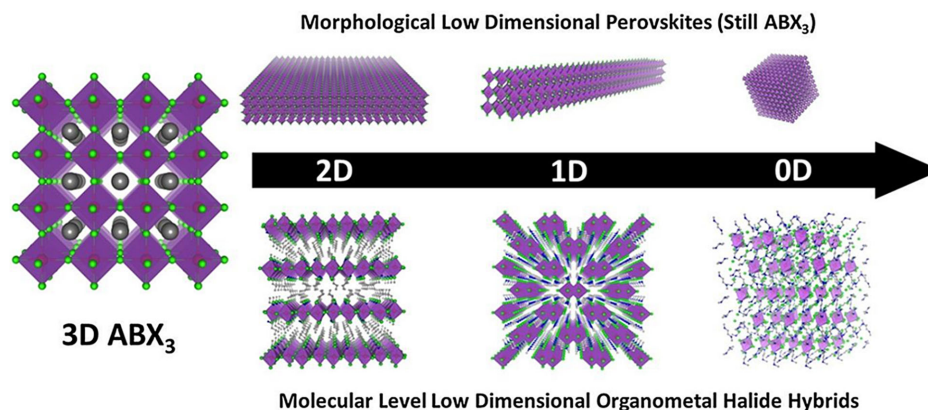
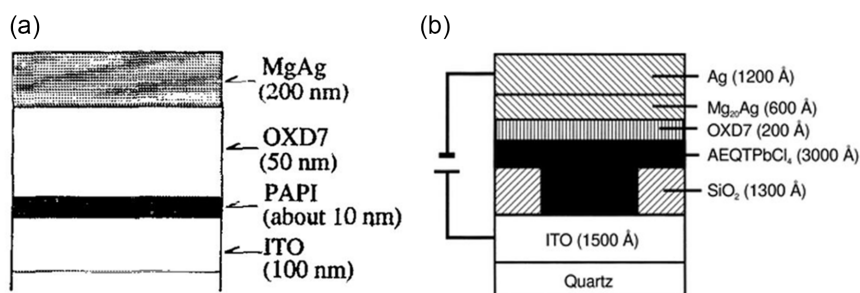


Figure 2
Self-assembled low-dimensional MHP MQWs before the Renaissance. (a) Low-temperature operating LED with phenethylammonium lead iodide (noted as PAPI, $(C_6H_5C_2H_4NH_3)_2PbI_4$) and (b) room temperature operating LED with AEQTPbCl₄ ($H_3NC_2H_4C_{16}H_8S_4C_2H_4NH_3PbCl_4$)



electrodes to complete electroluminescent device as shown in Figure 2(a). This device, however, could not operate in room temperature with notable performance; thus, the measurement went through low temperature formed by liquid nitrogen. As a result, they obtained 10,000 cd/m² luminance at high applied voltage of around 24 V. In the work by Chondroudis and Mitzi published after 5 years, AEQTPbCl₄ ($H_3NC_2H_4C_{16}H_8S_4C_2H_4NH_3PbCl_4$) were deposited in vacuum for PeLED as depicted in Figure 2(b) and operational in room temperature with reasonable turn-on voltage around 5 V and power conversion efficiency of 0.11%. These precious research works exhibit the high potential of 2D perovskite multiple quantum well (MQW) structure in optoelectronics field. However, the long organic chain in 2D perovskite MQWs hinders efficient charge transport, and this implies that there are several factors to optimize for practical application as the researchers have developed over a decade as below.

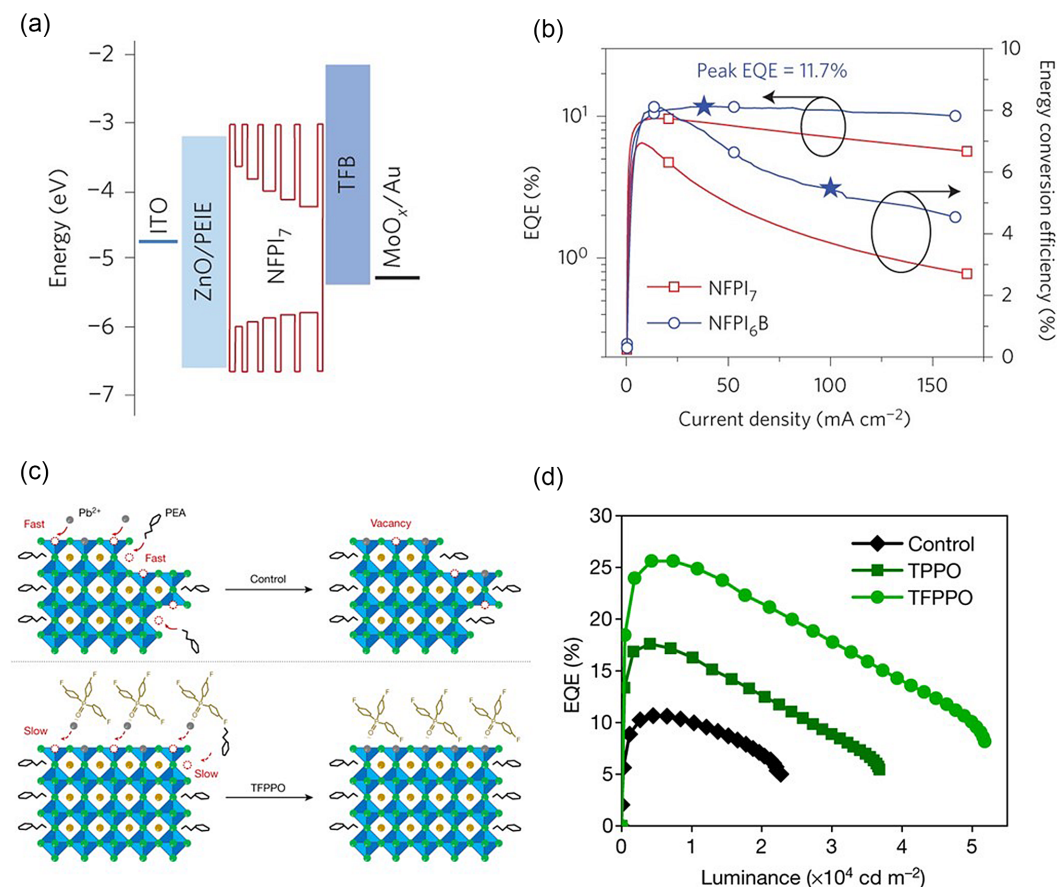
Since the Renaissance of perovskite optoelectronic devices in this century, the research groups over the world have achieved remarkable milestones using low dimensionality of MHPs [14, 15]. To fabricate typical high efficiency solar cells, bulky organic halides are spin-coated atop of 3D MHPs and form 2D/3D heterojunction structures. This 2D layers are able to protect 3D underlying perovskite light-absorbing layer from moisture or oxygen and decrease the interfacial charge carrier recombination between perovskite and upper charge transport layer. These

well-controlled 2D perovskite fabrications have remarkably improved perovskite solar cells that can harm charge extraction if the less conductive 2D layers are too thick. In case of LED research, the use of low-dimensional perovskite has been more direct since the high exciton binding energy and type-I heterojunction reinforce exciton recombination and ultimately light emission [16–23].

In 2016, a group in Nanjing Tech University led by Prof. Wei Huang reported highly efficient quasi-2D PeLEDs [24]. The schematic illustration in Figure 3(a) demonstrates the role of perovskite MQWs. They suggest that the contrasts in the perovskite layer reflect the vertical distributions of QWs with different $\langle n \rangle$. For instance, $n = 1$ and $n = \infty$ indicate completely molecular 2D perovskites and 3D perovskites, respectively, making the number between those as mixed dimensional phases. Perovskite QWs with higher $\langle n \rangle$ values accommodate more lead-halide octahedra per volume and confirm this with high-angle annular dark-field imaging. In other words, the majority of higher $\langle n \rangle$ QWs are in the regions close to the Perovskite/HTL (Poly(9,9-dioctylfluorene-alt-N-(4-sec-butylphenyl)-diphenylamine), TFB) interface. By the self-assembly of this MQW of quasi-2D MHPs, they could obtain world-record efficiency PeLEDs at that moment as Figure 3(b).

Recent report by Prof. Edward H. Sargent et al. gives a lesson regarding the way to control distribution by exploiting additives, not only the composition of perovskites [25–28]. For the fabrication of

Figure 3
Perovskite LEDs with perovskite MQW structures. (a) Early-stage perovskite MQW-based LEDs and (b) device efficiency as a function of current density. (c) Dimensional distribution-controlled perovskite MQW-based LEDs and (d) device efficiency as a function of luminance



perovskite MQW films, triphenylphosphine oxide (TPPO) and tris(4-fluorophenyl) phosphine oxide (TFPPO) additives are introduced in the anti-solvent which is injected into MHP films. Figure 3(c) shows the mechanism of improving crystal quality of perovskite. During anti-solvent-induced crystallization, lead bromide octahedral nuclei, methylammonium, and cesium cations assemble to form the perovskite flakes, allowing the bulky organic cations (PEA) to diffuse and enter the extended perovskite lattice, thereby forming quasi-2D perovskites. For the control film, rapid diffusion of PEA leads to MQW more inhomogeneous in molecular dimension, whereas TFPPO assists the crystallization with the fluorine atoms bind to PEA (hydrogen bonds), hindering their diffusion and enhancing the formation of quasi-2D with distribution-controlled MQWs. As a result, “Control” (without using any additive) and TPPO-treated perovskite MQW-based LEDs showed external quantum efficiencies (EQEs) of 10.7% and 17.6%, respectively, while TFPPO-treated perovskite MQW-based LEDs achieved an extremely high EQE of 25.6% as shown in Figure 3(d), which is already compatible with organic and quantum dot LEDs. This implies that MQWs with controlled dimension can be synthesized using a bi-functional molecular additive which controls the diffusion of the bulky organic PEA cations during crystal formation and also functioned as a surface passivators. In addition, the optoelectronic property of organic and inorganic blocks of hybrid perovskite building can be even more

sophistically controlled in single molecular scale as Gao et al. [29] reported. It was revealed that self-aggregation of the conjugated organic molecules is suppressed by functionalization with sterically demanding groups, and single crystalline organic-perovskite hybrid quantum wells (down to one-unit-cell thick) are obtained.

Moreover, the structural refinement could enhance overall performances of perovskite MQW LEDs. Ding et al. reported that a simple chemical washing method resolves the phase dimension issue of perovskite MQWs [30]. Their report deals with “solvent sieve treatment method” selectively which removes those undesirable low-*n* phases by mixing a polar solvent and non-polar anti-solvent together, and the treatment is performed by pouring mixed solvent directly onto perovskite films. Herein, the polar solvent serves as the mesh of the solvent sieve, interacting with perovskites, whereas the non-polar solvent serves as the framework part, without the sieving effect on perovskites. Due to their ionic crystal property, perovskites can be dissolved in some polar solvents but resist non-polar anti-solvents. A vast range of polar and non-polar solvent combinations can serve as solvent sieves. In one of the most efficient solvent sieve systems in this study (which consists of hexylamine (HA) and chlorobenzene), as the concentration of polar HA increases from 0 to 5%, the thickness of sifted film correspondingly decreases, implying that parts of the perovskite film are removed. After being sieved, undesirable defect-rich low-*n* phases are selectively screened out of perovskite MQW

structures, resulting in a remarkable EQE, current efficiency, and T_{50} lifetime of 29.5%, 127.4 cd A⁻¹, and 18.67 h at 12,000 cd m⁻² (the equivalent of over 50, 317 h or 5.7 years at 100 cd m⁻²).

This indicates that the control of n-value can realize extremely stable and efficient perovskite MQW devices, and there might be several more room to improve if this structural refinement techniques get improved. Yet, this refinement method in solution-based process is not well established. On the other hand, evaporating MHPs as a “well” and other materials as a “barrier” in MQWs remains simple and promising. Hence, suggested “artificial” fabrication of perovskite MQWs is introduced below.

3. Artificial Perovskite Multiple Quantum Wells

Perovskite MQWs have shown remarkable achievements in optoelectronic technologies, even if the formation of MQWs is self-assembly based. Research teams led by Prof. Osman Bakr and Prof. Omar F. Mohammed in King Abdullah University of Science and Technology have fabricated artificial MQWs by evaporating CsPbBr₃ and organic materials and investigated their properties [26–28].

For the artificial perovskite MQWs, the CsPbBr₃ perovskite single crystal is synthesized via inverse temperature crystallization and sequentially evaporated with 2,2',2''-(1,3,5-Benzinetriyl)-tris(1-phenyl-1-H-benzimidazole) (TPBi) as shown in Figure 4(a) [27]. It is noteworthy that the perovskite powder could be also mechanochemically synthesized, e.g., grinding and ball-milling [31, 32]. The time-of-flight secondary ion mass spectrometry data extracted from the MQW show this sequential evaporation makes proper boundaries of perovskite and organic material by separating each other (Figure 4(b)). Thus, in their report, it was possible to control the optical property of the perovskite layer as well by making different thicknesses offering quantum confinement as reported in Parrott et al. [33]. In addition, as shown in Figure 4(c)–(d), they could precisely control the thickness and exploit the full advantages of artificial perovskite MQW fabrication. Interestingly, MQWs made of different thickness of perovskite form asymmetric perovskite MQWs and proved by the PL spectra from all of the perovskite wells.

They also applied this MQW system to photodiode [28]. Not only TPBi as their previous report but also bathocuproine (BCP) is introduced to form various type of heterojunction. Due to the band gap alignment, TPBi-based MQW forms type-I structure and the BCP counterpart makes type-II. Both valance band maxima of TPBi and BCP are deeper than that of perovskite; however, conduction band minimum of TPBi is higher than that of perovskite and in case of BCP, the conduction band minimum is lower than that of perovskite. This fosters difference in electron extraction from perovskite; the current in 10⁻⁶ A in TPBi-based (Figure 4(e)) and 1 V is 10⁻³ A in BCP-based (Figure 4(f)) photodiode. In addition to this, the asymmetric perovskite MQWs show interesting properties such as the delayed hot carrier equilibrium mediated by the sequential hot-electron transfer between CsPbBr₃ layers inside of the asymmetric MQWs [26]. Moreover, a collaboration led by Prof. Henk J. Bolink in University of Valencia and Dr. Annamaria Petrozza in Italian Institute of Technology recently reported an amplified spontaneous emission (ASE) signal based on perovskite MQWs [34]. This highlights the possibility of perovskite MQW as an optical gain system for the future laser systems. Typical ASE occurs after amplification of light by the propagation inside of waveguide mode in the flat perovskite films [35]. To realize ASE in film, the certain thickness of gain material should be guaranteed and with the film should bear the high intensity of photoexcitation. By performing Williamson-Hall

analysis and extracting micro-strain value, the work with perovskite MQW found that the organic layer can stabilize the molecular dimension of 3D CsPbBr₃ and prevent the formation of molecular low-dimension (2D) CsPb₂Br₅ which has lower refractive index and confine less light, resulting in deformation of waveguide mode. In addition, the thickness of organic material must be optimized as shown in Figure 4(g). Decreased ASE signal by increasing TPBi thickness might be explained with enhanced internal reflection in thick TPBi layers, that can reinforce reabsorption in the perovskite in the multilayers thus increasing parasitic absorption [36]. To observe ASE, fast radiative recombination from a high charge carrier density is required; however, photon reabsorption redistributes the charge carriers and delays the recombination.

4. Next Optoelectronic and Photonic Research with Perovskite Multiple Quantum Wells

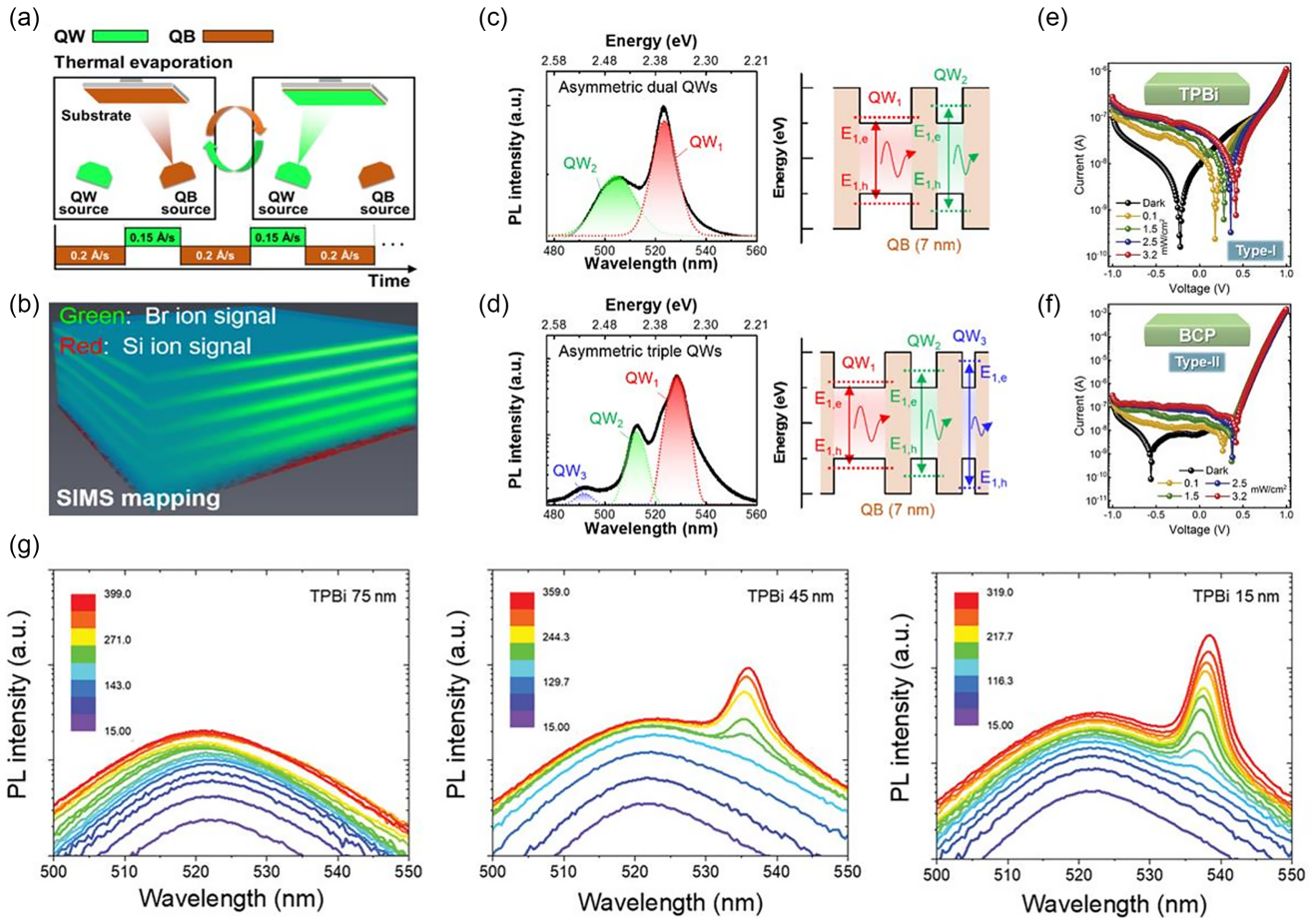
As described above, the observation of ASE signal indicates the potential of use in laser gain material. In a recent work led by Prof. Chihaya Adachi in Kyushu University, the first room temperature stable lasing emission by continuous-wave (CW) photoexcitation is reported. For this work, PEA and naphthylmethylamine (NMA) cations are introduced into formamidinium lead bromide perovskite forming quasi-2D MQW structure, and the perovskite is spin-coated onto SiO₂/Si distributed feedback cavity as shown in Figure 5(a)–(b) [37]. It is noteworthy to mention the effect of triplets on the population inversion during CW lasing was remarkable since the lasing intensity of PEA-perovskite MQWs immediately dropped when N₂ was injected into the sample chamber. Lasing was recovered completely after stopping the injection of nitrogen. On the other hand, the lasing intensity of NMA-perovskite MQWs decreased gradually because of its inferior stability. This observation implies that singlet–triplet exciton annihilation originating from long-lived triplet excitons is a possible intrinsic mechanism leading to CW lasing decrease in perovskites. Triplet excitons have been observed in 2D perovskites through intersystem crossing from singlet exciton states; however, the results demonstrate the role in the stimulated emission process and show the importance of managing triplet excitons in laser applications using quasi-2D perovskites.

Furthermore, as the “solvent sieving method” mentioned above, the extremely high stability and radiative recombination rate of structurally refined perovskite MQWs might be useful in this application as well. Furthermore, the combination of dimensional structure-refining technique by constructing artificial perovskite MQWs might be more beneficial to realize electrically pumped perovskite laser system due to the high stability in high density of radiative recombination [30].

In addition to lasing, recent works have demonstrated new perovskite light emitter called light-emitting electrochemical cells (LECs). Prof. Alan J. Heeger’s team in University of California, Santa Barbara campus, showed this system does not require transport layer between anodes and cathodes owing to the ionic dopants inside [38]. For MHPs, the Prof. Jason D. Slinker’s group in University of Texas, Dallas campus, have realized LECs with CsPbBr₃:poly(ethylene-oxide) (PEO) composite with LiPF₆ dopants [39–41]. However, this system indeed includes LiF interlayer between perovskite composite and metal electrode and requires long turn-on time over 1 hour. After several years, Prof. Henk J. Bolink’s group realized interlayer free CsPbBr₃:PEO composite LECs as shown in Figure 5(e) [42]. Interestingly, evaporated Cs₄PbCl₆, a molecularly OD, is employed to stabilize (Figure 5(f)) perovskite light emissive layer. This Chin-Sessolo-Bolink (CSB) junction exploits negligible solubility of Cs₄PbCl₆ in

Figure 4

Artificial perovskite MQW structures. (a) Fabrication process with CsPbBr_3 and organic material and (b) time-of-flight secondary ion mass spectrometry (TOF-SIMS) mapping image of artificial perovskite MQWs. Controllable energy alignment with asymmetric (c) dual and (d) triple perovskite QWs. Current–voltage characteristics of (e) type-I and (f) type-II perovskite MQWs. (g) Amplified spontaneous emission from perovskite MQWs as a function of the thickness of quantum barriers



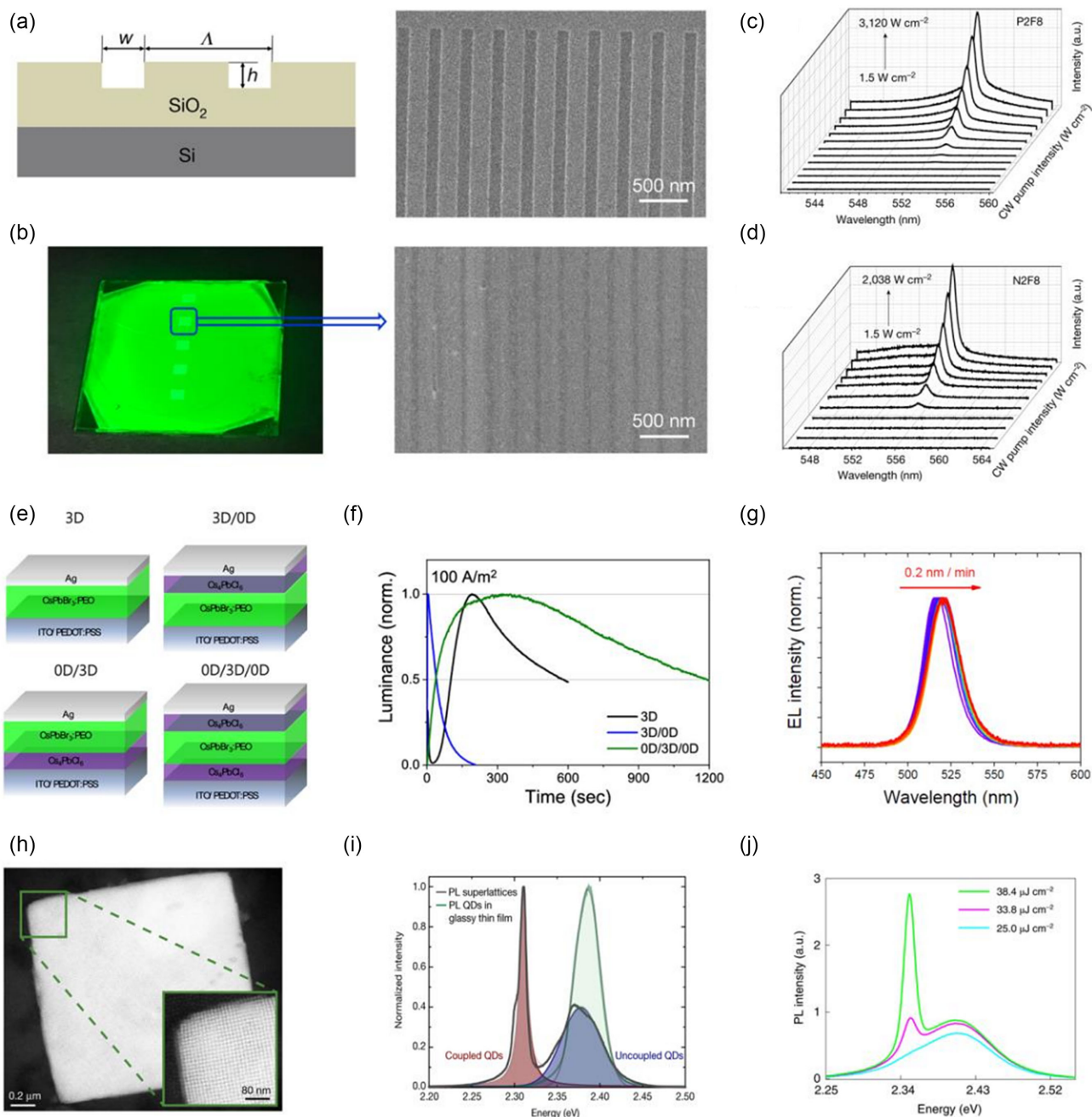
common solvents for MHPs such as DMSO and DMF. Owing to this, the layer could be introduced below and atop of perovskite layer as shown in Figure 5(g) without losing green luminescence from CsPbBr_3 :PEO composite. As a result, the bilateral intercalation of Cs_4PbCl_6 shows faster turn-on time and twice longer half lifetime. In addition, the small amount of intermixed chloride anion (which results in slight blue shift) moves towards electrode faster than bromide anion; hence, the emission peak has been restored as green by operating perovskite LECs. This CSB junction is just a single well system with 0D/3D/0D, but it might suggest the future application of artificial MQWs since the exploitation of orthogonality in solubility assists achievement of the multiple stacking.

Moreover, perovskite materials have been investigated for next-generation quantum technology. Prof. Maksym V. Kovalenko's team in ETH Zürich and IBM research center in Switzerland formed a superlattice of CsPbBr_3 quantum dots (Figure 5(h)) and observed the signal of super-fluorescence (SF) in 6K as shown in Figure 5(i) [43]. An ensemble of light emitters is able to show many-body interaction when they interact coherently via a common light field. After excitation of such an ensemble, collective coupling can give rise to a many-body quantum phenomenon that results in short, intense bursts of light. The research team confirms that this emission is SF after crosschecking Burnham-Chiao ringing in

time-resolved photoluminescence and second-order intensity correlation in Hanbury Brown-Twist setup. Also in North Carolina State University, Raleigh campus, Prof. Kenan Gundogdu's group exhibited SF in room temperature [44]. They simply spin-coated PEA-treated CsPbBr_3 quasi-2D MQWs and observed this signal as shown in Figure 5(j) despite the common SF research has been performed with small molecular or atomic cluster to prevent dephasing of quantum coherence such as gas or dopants in host. They claim the reason for this "extended electronic coherence" is the formation of large polarons [45, 46]. In perovskites, initial excitations lead to the formation of electron-hole pairs, but these excitations subsequently form polarons, by binding to a "lead-halide distortion mode" within a picosecond. It has been pointed out that the presence of these large polarons slows the hot carrier cooling rate by reducing thermal scattering and carrier-carrier scattering events. It is plausible that this strong coupling of the electronic dipoles to lattice distortion protects electronic coherence as well as facilitates the formation of a macroscopic coherent states for SF through a vibration isolation mechanism.

To properly use this SF phenomenon in perovskite MQW for practical applications, it might be necessary to refine the signal from ASE since the perovskite is already a nice optical gain material. With MHPs, such mixed phenomena or transition from

Figure 5
 Suggested next optoelectronic and photonic applications based on perovskite. (a) Distributed Bragg diffractor (DBR) and (b) perovskite MQWs deposited onto the DBR cavity. Room temperature stable continuous-wave lasing from laser excited (c) PEA-based and (d) NMA-based perovskite MQWs. (e) 0D/3D/0D perovskite single well light-emitting electrochemical cells and (f) improved stability with (g) maintained spectra by CSB junction. (h) Perovskite superlattice and (i) super-fluorescence from low temperature. (j) Room temperature super-fluorescence from perovskite MQWs



SF to ASE will be easily observed as reported by Malcuit et al. [47]. Since SF and ASE might be observed at the same time, the design of samples for SF should be opposed to that for ASE, and vice versa [35]. For example, to extract light and prevent waveguide mode propagation by internal reflection, the high refractive index of substrate will be suitable for SF.

In addition, the polaron in perovskite lattice can be controlled by employing charge transport materials [48]. For example, Prof. Feng Gao

and co-workers in Linköping University employed PTAA HTL under MAPbBr₃ perovskite for the observation of ASE. According to this report, the large polarons distort the lattice structure by Coulomb force. Thus, enhanced ionic vibration increases the phonon modes drastically, which increases the rate of phonon-assisted Auger recombination. By extracting the holes in perovskites, hot-hole relaxation will be facilitated, leading to reduced Auger loss, and thus favoring better optical gain property and enhanced ASE behavior.

The relatively slow hot-hole cooling process within the bare MAPbBr₃ film inevitably enlarges the ASE threshold and hinders the observation due to increased Auger loss [49–51]. By extracting the holes with PTAA, the cooling process is facilitated, which largely reduces the Auger loss and thus reduces the ASE threshold. As the example shows above, the double-side behavior of SF and ASE might be controlled via the modulation of polaron. Since the modulation of hot carrier cooling is available with artificial MQWs, there is full of future studies with perovskite MQW system for both fundamental scientific research and practical applications, spanning from conventional optoelectronics to quantum technologies [26, 52].

5. Conclusions

In this review, the remarkable progress in PeLEDs with quasi-2D MQW in efficiency and stability is introduced. In addition, the plausible advantage of employing perovskite MQWs into lasers, LECs and SF-observation are suggested. All these technologies might be further developed by controlling MQWs based on the understanding of nucleation dynamics of perovskite crystals and complexation with solvent or by employing artificial perovskite MQWs comprising organic barrier or inorganic barrier as the low-dimensional barrier included in CSB junction.

Ethical Statement

This study does not contain any studies with human or animal subjects performed by the author.

Conflicts of Interest

The author declares that he has no conflicts of interest to this work.

Data Availability Statement

Data sharing is not applicable to this article as no new data were created or analyzed in this study.

Author Contribution Statement

Sang-Hyun Chin: Conceptualization, Data curation, Writing – original draft, Writing – review & editing, Visualization, Supervision, Project administration.

References

- [1] Luo, J., Li, J., Grater, L., Guo, R., Mohd Yusoff, A. R. B., Sargent, E., & Tang, J. (2024). Vapour-deposited perovskite light-emitting diodes. *Nature Reviews Materials*, 9(4), 282–294. <https://doi.org/10.1038/s41578-024-00651-8>
- [2] Grätzel, M. (2017). The rise of highly efficient and stable perovskite solar cells. *Accounts of Chemical Research*, 50(3), 487–491. <https://doi.org/10.1021/acs.accounts.6b00492>
- [3] Rajagopal, A., Yao, K., & Jen, A. K. (2018). Toward perovskite solar cell commercialization: A perspective and research roadmap based on interfacial engineering. *Advanced Materials*, 30(32), e1800455. <https://doi.org/10.1002/adma.201800455>
- [4] Zhao, Y., Yavuz, I., Wang, M., Weber, M. H., Xu, M., Lee, J. H., . . . , & Yang, Y. (2022). Suppressing ion migration in metal halide perovskite via interstitial doping with a trace amount of multivalent cations. *Nature Materials*, 21(12), 1396–1402. <https://doi.org/10.1038/s41563-022-01390-3>
- [5] Zhou, C., Lin, H., He, Q., Xu, L., Worku, M., Chaaban, M., . . . , & Ma, B. (2019). Low dimensional metal halide perovskites and hybrids. *Materials Science and Engineering: R: Reports*, 137, 38–65. <https://doi.org/10.1016/j.mser.2018.12.001>
- [6] Kojima, A., Teshima, K., Shirai, Y., & Miyasaka, T. (2009). Organometal halide perovskites as visible-light sensitizers for photovoltaic cells. *Journal of the American Chemical Society*, 131(17), 6050–6051. <https://doi.org/10.1021/ja809598r>
- [7] Kim, H. S., Lee, C. R., Im, J. H., Lee, K. B., Moehl, T., Marchioro, A., . . . , & Park, N. G. (2012). Lead iodide perovskite sensitized all-solid-state submicron thin film mesoscopic solar cell with efficiency exceeding 9%. *Scientific Reports*, 2(1), 591. <https://doi.org/10.1038/srp00591>
- [8] Lee, M. M., Teuscher, J., Miyasaka, T., Murakami, T. N., & Snaith, H. J. (2012). Efficient hybrid solar cells based on meso-structured organometal halide perovskites. *Science*, 338(6107), 643–647. <https://doi.org/10.1126/science.1228604>
- [9] Tan, Z. K., Moghaddam, R. S., Lai, M. L., Docampo, P., Higler, R., Deschler, F., . . . , & Friend, R. H. (2014). Bright light-emitting diodes based on organometal halide perovskite. *Nature Nanotechnology*, 9(9), 687–692. <https://doi.org/10.1038/nnano.2014.149>
- [10] Deschler, F., Price, M., Pathak, S., Klüntberg, L. E., Jarausch, D. D., Higler, R., . . . , & Friend, R. H. (2014). High photoluminescence efficiency and optically pumped lasing in solution-processed mixed halide perovskite semiconductors. *The Journal of Physical Chemistry Letters*, 5(8), 1421–1426. <https://doi.org/10.1021/jz5005285>
- [11] Wells, H. L. (1893). Über die cäsium-und Kalium-Bleihalogenide [About the cesium and potassium lead halides]. *Journal of Inorganic and General Chemistry*, 3(1), 195–210. <https://doi.org/10.1002/zaac.18930030124>
- [12] Chondroudis, K., & Mitzi, D. B. (1999). Electroluminescence from an organic–inorganic perovskite incorporating a quaterthiophene dye within lead halide perovskite layers. *Chemistry of Materials*, 11(11), 3028–3030. <https://doi.org/10.1021/cm990561t>
- [13] Era, M., Morimoto, S., Tsutsui, T., & Saito, S. (1994). Organic-inorganic heterostructure electroluminescent device using a layered perovskite semiconductor (C₆H₅C₂H₄NH₃)₂PbI₄. *Applied Physics Letters*, 65(6), 676–678. <https://doi.org/10.1063/1.112265>
- [14] Bai, W., Xuan, T., Zhao, H., Dong, H., Cheng, X., Wang, L., & Xie, R. J. (2023). Perovskite light-emitting diodes with an external quantum efficiency exceeding 30%. *Advanced Materials*, 35(39), 2302283. <https://doi.org/10.1002/adma.202302283>
- [15] Yudco, S., & Etgar, L. (2024). Ruddlesden–Popper and Dion–Jacobson perovskites in multiple quantum wells light-emitting diodes. *Advanced Optical Materials*, 12(13), 2302592. <https://doi.org/10.1002/adom.202302592>
- [16] Ren, Z., Xiao, X., Ma, R., Lin, H., Wang, K., Sun, X. W., & Choy, W. C. (2019). Hole transport bilayer structure for quasi-2D perovskite based blue light-emitting diodes with high brightness and good spectral stability. *Advanced Functional Materials*, 29(43), 1905339. <https://doi.org/10.1002/adfm.201905339>
- [17] Liu, T., Jiang, Y., Qin, M., Liu, J., Sun, L., Qin, F., . . . , & Zhou, Y. (2019). Tailoring vertical phase distribution of quasi-two-dimensional perovskite films via surface modification of

- hole-transporting layer. *Nature Communications*, 10(1), 878. <https://doi.org/10.1038/s41467-019-08843-5>
- [18] Lei, L., Seyitliyev, D., Stuard, S., Mendes, J., Dong, Q., Fu, X., . . . , & So, F. (2020). Efficient energy funneling in quasi-2D perovskites: From light emission to lasing. *Advanced Materials*, 32(16), 1906571. <https://doi.org/10.1002/adma.201906571>
- [19] Leung, T. L., Ahmad, I., Syed, A. A., Ng, A. M. C., Popović, J., & Djurišić, A. B. (2022). Stability of 2D and quasi-2D perovskite materials and devices. *Communications Materials*, 3(1), 63. <https://doi.org/10.1038/s43246-022-00285-9>
- [20] Kumar, G. S., Sumukam, R. R., & Murali, B. (2020). Quasi-2D perovskite emitters: A boon for efficient blue light-emitting diodes. *Journal of Materials Chemistry C*, 8(41), 14334–14347. <https://doi.org/10.1039/D0TC03471A>
- [21] Zhang, L., Sun, C., He, T., Jiang, Y., Wei, J., Huang, Y., & Yuan, M. (2021). High-performance quasi-2D perovskite light-emitting diodes: From materials to devices. *Light: Science & Applications*, 10(1), 61. <https://doi.org/10.1038/s41377-021-00501-0>
- [22] Yuan, M., Quan, L. N., Comin, R., Walters, G., Sabatini, R., Voznyy, O., . . . , & Sargent, E. H. (2016). Perovskite energy funnels for efficient light-emitting diodes. *Nature Nanotechnology*, 11(10), 872–877. <https://doi.org/10.1038/nnano.2016.110>
- [23] Yang, X., Zhang, X., Deng, J., Chu, Z., Jiang, Q., Meng, J., . . . , & You, J. (2018). Efficient green light-emitting diodes based on quasi-two-dimensional composition and phase engineered perovskite with surface passivation. *Nature Communications*, 9(1), 570. <https://doi.org/10.1038/s41467-018-02978-7>
- [24] Wang, N., Cheng, L., Ge, R., Zhang, S., Miao, Y., Zou, W., . . . , & Huang, W. (2016). Perovskite light-emitting diodes based on solution-processed self-organized multiple quantum wells. *Nature Photonics*, 10(11), 699–704. <https://doi.org/10.1038/nphoton.2016.185>
- [25] Ma, D., Lin, K., Dong, Y., Choubisa, H., Proppe, A. H., Wu, D., . . . , & Sargent, E. H. (2021). Distribution control enables efficient reduced-dimensional perovskite LEDs. *Nature*, 599(7886), 594–598. <https://doi.org/10.1038/s41586-021-03997-z>
- [26] Maity, P., Merdad, N. A., Yin, J., Lee, K. J., Sinatra, L., Bakr, O. M., & Mohammed, O. F. (2021). Cascade electron transfer induces slow hot carrier relaxation in CsPbBr₃ asymmetric quantum wells. *ACS Energy Letters*, 6(7), 2602–2609. <https://doi.org/10.1021/acsenenergylett.1c01142>
- [27] Lee, K. J., Turedi, B., Sinatra, L., Zhumekenov, A. A., Maity, P., Dursun, I., . . . , & Bakr, O. M. (2019). Perovskite-based artificial multiple quantum wells. *Nano Letters*, 19(6), 3535–3542. <https://doi.org/10.1021/acs.nanolett.9b00384>
- [28] Lee, K. J., Merdad, N. A., Maity, P., El-Demellawi, J. K., Lui, Z., Sinatra, L., . . . , & Bakr, O. M. (2021). Engineering band-type alignment in CsPbBr₃ perovskite-based artificial multiple quantum wells. *Advanced Materials*, 33(17), 2005166. <https://doi.org/10.1002/adma.202005166>
- [29] Gao, Y., Shi, E., Deng, S., Shiring, S. B., Snaider, J. M., Liang, C., . . . , & Dou, L. (2019). Molecular engineering of organic–inorganic hybrid perovskites quantum wells. *Nature chemistry*, 11(12), 1151–1157. <https://doi.org/10.1038/s41557-019-0354-2>
- [30] Ding, S., Wang, Q., Gu, W., Tang, Z., Zhang, B., Wu, C., . . . , & Xiang, C. (2024). Phase dimensions resolving of efficient and stable perovskite light-emitting diodes at high brightness. *Nature Photonics*, 18(4), 363–370. <https://doi.org/10.1038/s41566-023-01372-0>
- [31] El Ajjouri, Y., Chirvony, V. S., Vassilyeva, N., Sessolo, M., Palazon, F., & Bolink, H. J. (2019). Low-dimensional non-toxic A₃Bi₂X₉ compounds synthesized by a dry mechanochemical route with tunable visible photoluminescence at room temperature. *Journal of Materials Chemistry C*, 7(21), 6236–6240. <https://doi.org/10.1039/C9TC01765H>
- [32] Palazon, F., El Ajjouri, Y., Sebastia-Luna, P., Lauciello, S., Manna, L., & Bolink, H. J. (2019). Mechanochemical synthesis of inorganic halide perovskites: Evolution of phase-purity, morphology, and photoluminescence. *Journal of Materials Chemistry C*, 7(37), 11406–11410. <https://doi.org/10.1039/C9TC03778K>
- [33] Parrott, E. S., Patel, J. B., Haghhighrad, A. A., Snaith, H. J., Johnston, M. B., & Herz, L. M. (2019). Growth modes and quantum confinement in ultrathin vapour-deposited MAPbI₃ films. *Nanoscale*, 11(30), 14276–14284. <http://doi.org/10.1039/C9NR04104D>
- [34] Chin, S. H., Cortecchia, D., Forzatti, M., Wu, C. S., Alvarado-Leaños, A. L., Folpini, G., . . . , & Bolink, H. J. (2024). Stabilizing single-source evaporated perovskites with organic interlayers for amplified spontaneous emission. *Advanced Optical Materials*, 12(13), 2302701. <https://doi.org/10.1002/adom.202302701>
- [35] Cho, C., Palatnik, A., Sudzius, M., Grodofzig, R., Nehm, F., & Leo, K. (2020). Controlling and optimizing amplified spontaneous emission in perovskites. *ACS Applied Materials & Interfaces*, 12(31), 35242–35249. <https://doi.org/10.1021/acsmi.0c08870>
- [36] Navarro-Arenas, J., Suárez, I., Chirvony, V. S., Gualdrón-Reyes, A. F., Mora-Seró, I., & Martínez-Pastor, J. (2019). Single-exciton amplified spontaneous emission in thin films of CsPbX₃ (X = Br, I) perovskite nanocrystals. *The Journal of Physical Chemistry Letters*, 10(20), 6389–6398. <https://doi.org/10.1021/acs.jpcclett.9b02369>
- [37] Qin, C., Sandanayaka, A. S., Zhao, C., Matsushima, T., Zhang, D., Fujihara, T., & Adachi, C. (2020). Stable room-temperature continuous-wave lasing in quasi-2D perovskite films. *Nature*, 585(7823), 53–57. <https://doi.org/10.1038/s41586-020-2621-1>
- [38] Pei, Q., Yu, G., Zhang, C., Yang, Y., & Heeger, A. J. (1995). Polymer light-emitting electrochemical cells. *Science*, 269(5227), 1086–1088. <https://doi.org/10.1126/science.269.5227.1086>
- [39] Mishra, A., Alahbakhshi, M., Gu, Q., Zakhidov, A. A., & Slinker, J. D. (2021). Leveraging a stable perovskite composite to satisfy blue electroluminescence standards. *ACS Materials Letters*, 3(9), 1357–1362. <https://doi.org/10.1021/acsmaterialslett.1c00404>
- [40] Mishra, A., Alahbakhshi, M., Haroldson, R., Bastatas, L. D., Gu, Q., Zakhidov, A. A., & Slinker, J. D. (2020). Enhanced operational stability of perovskite light-emitting electrochemical cells leveraging ionic additives. *Advanced Optical Materials*, 8(13), 2000226. <https://doi.org/10.1002/adom.202000226>
- [41] Alahbakhshi, M., Mishra, A., Haroldson, R., Ishteev, A., Moon, J., Gu, Q., . . . , & Zakhidov, A. A. (2019). Bright and effectual perovskite light-emitting electrochemical cells leveraging ionic additives. *ACS Energy Letters*, 4(12), 2922–2928. <https://doi.org/10.1021/acsenenergylett.9b01925>
- [42] Chin, S. H., Mardegan, L., Palazon, F., Sessolo, M., & Bolink, H. J. (2022). Dimensionality controls anion intermixing in electroluminescent perovskite heterojunctions. *ACS*

- Photonics*, 9(7), 2483–2488. <https://doi.org/10.1021/acsp Photonics.2c00604>
- [43] Rainò, G., Becker, M. A., Bodnarchuk, M. I., Mahrt, R. F., Kovalenko, M. V., & Stöferle, T. (2018). Superfluorescence from lead halide perovskite quantum dot superlattices. *Nature*, 563(7733), 671–675. <https://doi.org/10.1038/s41586-018-0683-0>
- [44] Biliroglu, M., Findik, G., Mendes, J., Seyitliyev, D., Lei, L., Dong, Q., . . . , & Gundogdu, K. (2022). Room-temperature superfluorescence in hybrid perovskites and its origins. *Nature Photonics*, 16(4), 324–329. <https://doi.org/10.1038/s41566-022-00974-4>
- [45] Zhu, X. Y., & Podzorov, V. (2015). Charge carriers in hybrid organic–inorganic lead halide perovskites might be protected as large polarons. *The Journal of Physical Chemistry Letters*, 6(23), 4758–4761. <https://doi.org/10.1021/acs.jpcllett.5b02462>
- [46] Srimath Kandada, A. R., & Silva, C. (2020). Exciton polarons in two-dimensional hybrid metal-halide perovskites. *The Journal of Physical Chemistry Letters*, 11(9), 3173–3184. <https://doi.org/10.1021/acs.jpcllett.9b02342>
- [47] Malcuit, M. S., Maki, J. J., Simkin, D. J., & Boyd, R. W. (1987). Transition from superfluorescence to amplified spontaneous emission. *Physical Review Letters*, 59(11), 1189. <https://doi.org/10.1103/PhysRevLett.59.1189>
- [48] Zhang, J., Qin, J., Cai, W., Tang, Y., Zhang, H., Wang, T., . . . , & Gao, F. (2023). Transport layer engineering toward lower threshold for perovskite lasers. *Advanced Materials*, 35(30), 2300922. <https://doi.org/10.1002/adma.202300922>
- [49] Chen, J., Messing, M. E., Zheng, K., & Pullerits, T. (2019). Cation-dependent hot carrier cooling in halide perovskite nanocrystals. *Journal of the American Chemical Society*, 141(8), 3532–3540. <https://doi.org/10.1021/jacs.8b11867>
- [50] Li, M., Fu, J., Xu, Q., & Sum, T. C. (2019). Slow hot-carrier cooling in halide perovskites: Prospects for hot-carrier solar cells. *Advanced Materials*, 31(47), 1802486. <https://doi.org/10.1002/adma.201802486>
- [51] Joshi, P. P., Machrlein, S. F., & Zhu, X. (2019). Dynamic screening and slow cooling of hot carriers in lead halide perovskites. *Advanced Materials*, 31(47), 1803054. <https://doi.org/10.1002/adma.201803054>
- [52] White, L. R., Kosasih, F. U., Sherburne, M. P., Mathews, N., Mhaisalkar, S., & Bruno, A. (2024). Perovskite multiple quantum well superlattices: Potentials and challenges. *ACS Energy Letters*, 9(3), 835–842. <https://doi.org/10.1021/acscenrgylett.3c02612>

How to Cite: Chin, S.-H. (2024). Artificial Perovskite Multiple Quantum Well Optoelectronics. *Journal of Optics and Photonics Research*. <https://doi.org/10.47852/bonviewJOPR42022936>